ABSTRACT: Reducing-body myopathy (RBM) is a rare myopathy characterized by the presence of unique sarcoplasmic inclusions called reducing bodies (RBs). We characterized the aggresomal features of RBs that contained γ–tubulin, ubiquitin, and endoplasmic reticulum (ER) chaperones, together with a set of membrane proteins, in a family with hereditary RBM. Increased messenger ribonucleic acid and protein levels of a molecular chaperone, glucose-related protein 78, were also observed. These results suggest that the unfolded protein response caused by the accumulation of misfolded proteins in the endoplasmic reticulum plays an important role in the formation of RBs.

Muscle Nerve **35:** 322–326, 2007

UNFOLDED PROTEIN RESPONSE AND AGGRESOME FORMATION IN HEREDITARY REDUCING-BODY MYOPATHY

TEERIN LIEWLUCK, MD,[1] YUKIKO K. HAYASHI, MD, PhD,[1] MAKI OHSAWA, MD,[2] RUMI KUROKAWA, BS,[1] MASAKO FUJITA, BS,[1] SATORU NOGUCHI, PhD,[1] IKUYA NONAKA, MD, PhD,[1] and ICHIZO NISHINO, MD, PhD[1]

[1] Department of Neuromuscular Research, National Institute of Neuroscience, National Center of Neurology and Psychiatry, 4-1-1 Ogawa-Higashi, Kodaira, Tokyo 187-8502, Japan
[2] Department of Child Neurology, National Center Hospital for Mental, Nervous and Muscular Disorders, National Center of Neurology and Psychiatry, Tokyo, Japan

Accepted 26 September 2006

The endoplasmic reticulum (ER) is the site where newly synthesized secretory and membrane proteins are folded and assembled under a stringent quality-control system that prevents the development of aberrant conformers. The accumulation of misfolded/unfolded proteins in the ER leads to the unfolded protein response (UPR) that enhances folding capacity by transcriptional induction of ER chaperones and translationally represses protein synthesis. Misfolded proteins are removed from the ER by retrotranslocation to the cytosol and degradation by the ubiquitin–proteasome system.[9] If these misfolded proteins fail to fold correctly and are not degraded by the proteasome, they are transported in a microtubule-dependent manner to the perinuclear microtubule-organizing center together with ubiquitin, ER chaperones, and form cytoplasmic aggregates called aggresomes.[8] Aggresomes are usually surrounded by a cage of reorganized intermediate filaments and undergo autophagolysosomal degradation.[8] Postmitotic cells, such as neurons and myocytes, are particularly vulnerable to the detrimental effects of aggresome accumulation because they cannot reduce potentially toxic substances through cell division.[9]

Reducing-body myopathy (RBM) is a rare myopathy characterized pathologically by the presence of intracytoplasmic inclusion bodies strongly stained by menadione-linked α-glycerophosphate dehydrogenase (MAG) in the absence of substrate, α-glycerophosphate.[1] The term "reducing body (RB)" implies the reducing activity of the inclusions to nitroblue tetrazolium in the absence of substrate. This condition is also commonly associated with rimmed vacuoles and cytoplasmic bodies. The clinical features of RBM are variable and can be classified into three forms, namely (1) severe infantile form,[1,8] (2) benign congenital form,[13] and (3) late onset form.[2]

This article includes Supplementary Material available via the internet at http://www.mrw.interscience.wiley.com/suppmat/0148-639X/suppmat/

Abbreviations: endoplasmic reticulum stress-associated degradation; G3PDH, glyceraldehyde-3-phosphate dehydrogenase; GRP, glucose-regulated protein; ER, endoplasmic reticulum; hRBM, hereditary reducing body myopathy; IBMPFD, inclusion body myopathy associated with Paget's disease of bone and frontotemporal dementia; MAG, menadione-linked α-glycerophosphate dehydrogenase; mRNA, messenger ribonucleic acid; RB, reducing-body; RBM, reducing-body myopathy; RT-PCR, reverse transcriptase-polymerase chain reaction; sRBM, sporadic reducing-body myopathy; UPR, unfolded protein response; VCP, valosin-containing protein

Key words: aggresome; endoplasmic reticulum stress; endoplasmic reticulum stress-associated degradation (ERAD); reducing-body myopathy; unfolded protein response

Correspondence to: Y. K. Hayashi; e-mail: hayas_y@ncnp.go.jp

Published online 10 November 2006 in Wiley InterScience (www.interscience.wiley.com). DOI 10.1002/mus.20691

Table 1. Results of immunoreaction of reducing body (RB) in the hereditary RB myopathy (hRBM) muscle.

Protein category	Immunoreactivity	
	Positive	Negative
Nucleoplasm	None	Nuclei, nucleoli
Nuclear envelope	Emerin, Lamin A, Lamin C, LAP2	Lamin B
Centrosome	γ-tubulin (C)	None
UPR	IRE1α, p-PERK, GRP78, GRP94, Calnexin, ERp72, PDI	None
ERAD	VCP, Polyubiquitin, 26S proteasome P27 subunit (P)	None
Cytoplasmic chaperones	HSP70	αB crystallin
Internal membranes	GM130, Limp1, LAMP2, SERCA1, SERCA2	None
Intermediate filaments	Desmin (P)	None
Sarcomere	Actin (P)	α-actinin, MHC fast, MHC slow, Titin, Telethonin
Plasma membrane	Dystrophin, α-, β-DG, α-SG, Dysferlin, Caveolin-3, nNOS, Integrin α7B, ILK, Paxillin,	None
Basal lamina and extracellular matrix	None	Merosin, Collagen VI
Others	Caspase-3, Polyglutamine	Neurofilament, Plectin, β amyloid 1-40, 1-42

UPR, unfolded protein response; ERAD, endoplasmic reticulum stress-associated degradation; C, central staining of RB; VCP, valosin-containing protein; P, peripheral staining of RB.

Most of the patients have sporadic disease and only a few familial cases have been reported.[4,7] Here we report the aggresomal features of RBs found in a new family with hereditary RBM (hRBM).

MATERIALS AND METHODS

Patients. Details of the clinical features of this family with hRBM have been described elsewhere.[11] Briefly, patient 1 is an 11-year-old boy of Japanese and Filipino descent in good health until 10 years of age, when he developed proximal-dominant muscle weakness and spinal rigidity. Serum creatine kinase was elevated to 495 IU/L (normal <70 IU/L), and a muscle biopsy was performed from the left biceps brachii at 11 years of age. Patient 2 is the mother of patient 1, a 35-year-old Filipino. She noticed asymmetrical generalized muscle weakness at 29 years of age and became wheelchair-bound 5 years later. No spinal rigidity was observed. Serum creatine kinase level was elevated to 417 IU/L, and muscle biopsy was performed at the age of 31 years.

Muscle specimens from both patients displayed scattered MAG-positive cytoplasmic inclusions in the absence of substrate, α-glycerophosphate. Some muscle fibers contained rimmed vacuoles. Atrophic fibers that partly clustered in groups and scattered cytoplasmic bodies were also seen in the specimen from patient 1. On electron microscopy, RBs frequently engulfed myonuclei and consisted of clusters of granular materials with electron density similar to chromatin.

Immunohistochemical and Western Blot Analyses. The antibodies used in this study are listed in the table which appears as supplementary material athttp://www.mrw.interscience.wiley.com/suppmat/0148-639X/suppmat/. Immunohistochemical and Western blot analyses were performed as previously described.[6] The sections were incubated overnight with primary antibodies at 4°C. Immunostaining was also performed using muscle specimens from two previously reported patients with a severe, sporadic infantile form of RBM (sRBM).[8]

Quantitative RT-PCR. Total ribonucleic acid was extracted from frozen muscles of patient 1, one sRBM, and three age-matched controls as previously described.[8] Quantitative reverse transcriptase–polymerase chain reaction (RT-PCR) was performed using iCycler (Bio-Rad Laboratories, Richmond, California) adhering to the manufacturer's protocol. Primer sequences for the 78-kDa glucose-regulated protein (*GRP78*) gene (F: 5′-GTGGTAGTGCAAGCTGAAGG; R: 5′-TGGAGTCTCACTCTTGTCGC) and glyceraldehyde-3-phosphate dehydrogenase (*G3PDH*) gene (F: 5′-GGTAAAGTGGATATTGTTGCCATCAATG; R: 5′-GGAGGGATCTCGCTCCTGGAAGATGGTG) were used. The values of GRP78 mRNA were normalized to that of G3PDH.

Mutation Analysis. Genomic deoxyribonucleic acid was isolated from peripheral lymphocytes using a standard technique. Sequence analysis of the valosin-containing protein (*VCP*) gene was directly performed using ABI PRISM 3100 automated sequencer (Applied Biosystems Japan, Tokyo, Japan). Informazhy;eb;njtion on primer sequence and condi-

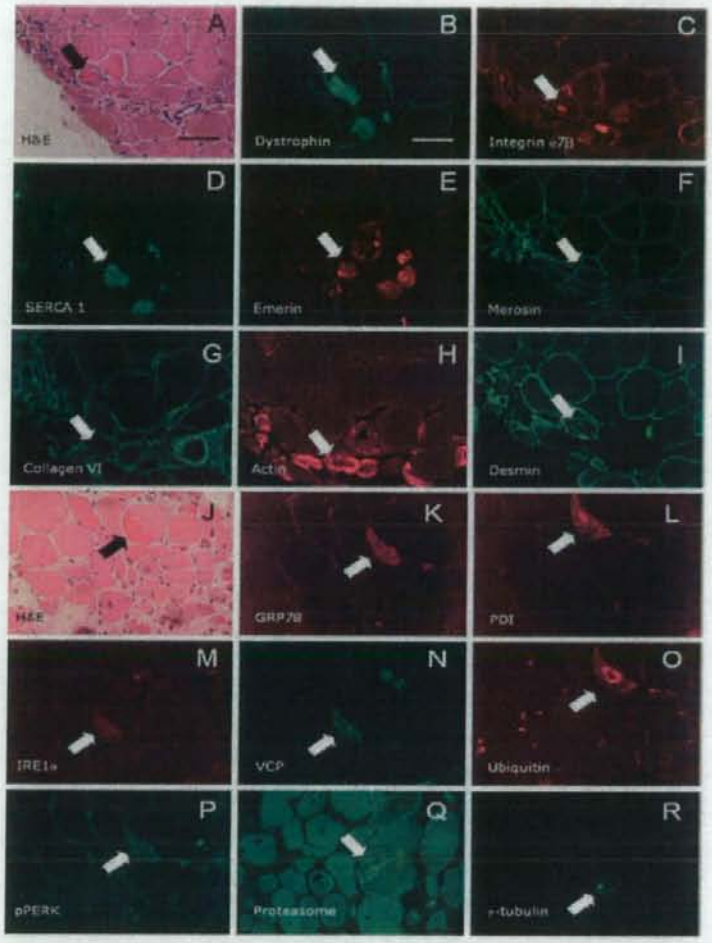

FIGURE 1. Immunohistochemical features of reducing bodies (RBs, arrows) in patient 1. **(A–I)** and **(J–R)** are serial sections. RBs appears as brightly eosinophilic sarcoplasmic inclusion on hematoxylin and eosin **(A,J)**. Various plasma membrane proteins such as dystrophin **(B)** and integrin α7B **(C)** as well as internal membrane protein SERCA1 **(D)** and nuclear membrane protein, emerin **(E)** are present in RBs. No immunoreactivity for extracellular matrix proteins including merosin **(F)** and collagen VI **(G)** is seen. Actin **(H)** and desmin **(I)** occasionally form a cage encircling RBs. RBs are also highlighted by antibodies against unfolded protein response-related molecules such as GRP78 **(K)**, PDI **(L)**, and IRE1α **(M)**, as well as ERAD-related proteins including VCP **(N)** and polyubiquitin **(O)**. Immunoreactivity of p-PERK **(P)**, an active form of PERK, confirms the activation of unfolded protein response. Proteasome **(Q)** stains only the periphery of reducing body while γ-tubulin **(R)** predominantly marks its center. Scale bar, 40 μm.

tions of polymerase chain reaction are available upon request.

RESULTS

Immunohistochemical and Western Blot Analyses. RBs were strongly stained for the various antibodies used in the muscles from hRBM (Table 1, Fig. 1). Serial sections revealed that larger-sized RBs showed positive immunoreactions for polyubiquitin, ER chaperones, membrane-associated proteins, nuclear envelope proteins, and caspase-3. The periphery of the RBs was immunoreactive for the proteasome P27 subunit, actin, and desmin, and the center of the RBs was immunoreactive for γ-tubulin, a centrosome-specific tubulin. Immunoblotting analysis revealed an increased amount of

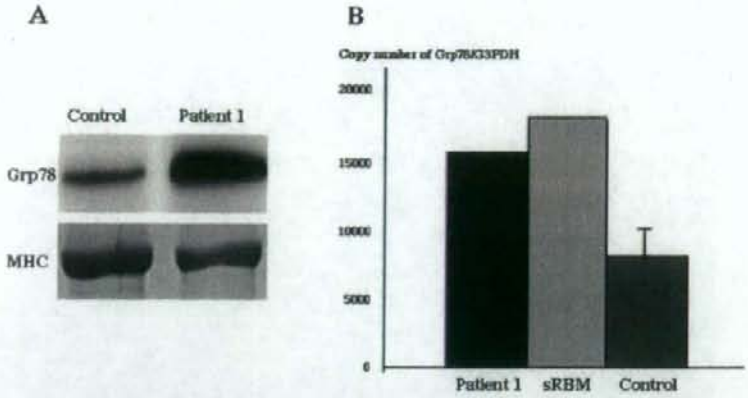

FIGURE 2. (A) Immunoblotting analysis of GRP78. More intense immunoreactive band for GRP78 is seen in patient 1. MHC: myosin heavy chain. **(B)** Histogram represents the results of quantitative RT-PCR for GRP78 on muscle biopsies. GRP78 in patient 1 and a sporadic reducing-body myopathy (sRBM) patient is upregulated compared to the control samples.

GRP78 expression in muscle from patient 1 compared to the control muscle (Fig. 2A).

Quantitative RT-PCR. The expression of GRP78 mRNA was much higher in the muscles from both patient 1 and one sRBM than the control muscles (Fig. 2B).

Mutation Analysis. No mutation was identified in the *VCP* gene in either patient 1 or 2.

DISCUSSION

Recently, aggresomal features of the inclusion bodies have been reported in several neurodegenerative disorders including Huntington's and Parkinson's diseases. Inclusions observed in Huntington's disease are specifically composed of mutant huntingtin together with ER chaperones and ubiquitin, whereas α-synuclein is the major component in Lewy bodies observed in Parkinson's disease.[9]

In this study, we demonstrated that RBs observed in hRBM patients contained virtually all membrane-associated proteins examined including those of nuclei, sarcoplasmic reticulum, Golgi apparatus, lysosome, and plasma membrane. RBs also had aggresomal features; i.e., positive immunoreaction for ubiquitin and ER chaperones, and positive central immunoreaction for γ-tubulin, and were surrounded by desmin, a major intermediate filament protein of skeletal muscle. Furthermore, increased mRNA and protein levels of GRP78 were observed in the muscle from the hRBM patient. GRP78 is a molecular chaperone, which is upregulated during UPR. Positive immunoreaction for phosphorylated (activated) pancreatic ER kinase observed in RBs also indicates the activation of UPR. From these results, accumulation of various misfolded membrane proteins in ER could be a primary event in hRBM patients, which results in activation of the UPR and subsequent aggresome formation. γ-Tubulin is a marker of the centrosome. Although postmitotic cells like muscle fibers and neurons normally do not contain a centrosome, γ-tubulin distinctly exists in the cytosol. In neurons, the cytosolic γ-tubulins could be reorganized to form juxtanuclear condensation under ER stress, and this lesion could be the microtubule organization center.[9] Positive immunoreaction for γ-tubulin in the center of RBs also suggests ER stress in hRBM.

Except for the consistency of ubiquitin immunoreactivity, previous reports showed equivocal immunohistochemical results of RBs.[2] To know whether the present results could apply to other patients with RBM, we also examined muscle specimens from two sRBM patients with the severe infantile form of the disease. All RBs found in sRBM patients yielded positive immunoreactivity of GRP78, ubiquitin, and emerin, but only a subset of RBs was highlighted by dystrophin and α-sarcoglycan. A desmin-positive rim was not seen in RBs in the sRBM muscles. Deposition of the proteins associated with UPR and ER-associated degradation, together with upregulation of GRP78 mRNA also indicates the activation of UPR in sRBM muscle samples.

Recently, a mutation in the *VCP* gene, a key molecule in the retrotranslocation step of ER stress-associated degradation, was identified in patients with inclusion-body myopathy associated with Paget's disease of bone and frontotemporal dementia (IBMPFD).[14] Due to the similarity of VCP-positive inclusions observed in the hRBM to that in IBMPFD, sequence analysis of the *VCP* gene was performed. However, no mutation was identified in the patients with hRBM.

In conclusion, our data show the aggresomal features of RBs, which might be induced by accumulation of a battery of membrane-associated proteins, resulting in the activation of UPR. To determine the precise pathomechanism of RBM, detailed analyses on the functions of ER chaperones and proteasomes should be investigated. In animal studies, overexpression of chaperones or application of chaperone-inducing compounds such as radicicol is beneficial for the treatment of neurodegenerative diseases with inclusion bodies.[9] Upregulation of chaperone transcription may be an option for the development of therapy in RBM.

We thank Dr. A. Kakizuka (Kyoto University, Japan) for providing the antibody for VCP, and Dr. M. Astejada (National Institute of Neuroscience, Tokyo, Japan) for reviewing the article. This work was supported by the Research on Health Sciences focusing on Drug Innovation from the Japanese Health Sciences Foundation; by the Research on Psychiatric and Neurological Diseases and Mental Health of Health and Labor Sciences research grants and the research grant (17A-10) for nervous and mental disorders from the Ministry of Health, Labor and Welfare; by a Grant-in-Aid for Scientific Research from the Japan Society for the Promotion of Science; and by the Program for Promotion of Fundamental Studies in Health Sciences of the National Institute of Biomedical Innovation.

REFERENCES

1. Brooke MH, Neville HE. Reducing body myopathy. Neurology 1972;22:829–840.
2. Figarella-Branger D, Putzu GA, Bouvier-Labit C, Pouget J, Chateau D, Fardeau M, et al. Adult onset reducing body myopathy. Neuromuscul Disord 1999;9:580–586.
3. Garcia-Mata R, Gao YS, Sztul E. Hassles with taking out the garbage: aggravating aggresomes. Traffic 2002;3:388–396.
4. Goebel HH, Halbig LE, Goldfarb L, Schober R, Albani M, Neuen-Jacob E, et al. Reducing body myopathy with cytoplasmic bodies and rigid spine syndrome: a mixed congenital myopathy. Neuropediatrics 2001;32:196–205.
5. Hayashi YK, Chou FL, Engvall E, Ogawa M, Matsuda C, Hirabayashi S, et al. Mutations in the integrin alpha7 gene cause congenital myopathy. Nat Genet 1998;19:94–97.
6. Hayashi YK, Ogawa M, Tagawa K, Noguchi S, Ishihara T, Nonaka I, et al. Selective deficiency of alpha-dystroglycan in Fukuyama-type congenital muscular dystrophy. Neurology 2001;57:115–121.
7. Hubner G, Pongratz D. Reducing body myopathy—ultrastructure and classification. Virchows Arch A Pathol Anat Histol 1981;392:97–104.
8. Kiyomoto BH, Murakami N, Kobayashi Y, Nihei K, Tanaka T, Takeshita K, et al. Fatal reducing body myopathy. Ultrastructural and immunohistochemical observations. J Neurol Sci 1995;128:58–65.
9. Muchowski PJ, Wacker JL. Modulation of neurodegeneration by molecular chaperones. Nat Rev Neurosci 2005;6:11–22.
10. Noguchi M, Takata T, Kimura Y, Manno A, Murakami K, Koike M, et al. ATPase activity of p97/valosin-containing protein is regulated by oxidative modification of the evolutionally conserved cysteine 522 residue in Walker A motif. J Biol Chem 2005;280:41332–41341.
11. Ohsawa M, Liewluck T, Ogata K, Iizukad T, Hayashi Y, Nonaka I, et al. Familial reducing body myopathy. Brain Dev (in press).
12. Sakaki M, Koike H, Takahashi N, Sasagawa N, Tomioka S, Arahata K, et al. Interaction between emerin and nuclear lamins. J Biochem (Tokyo) 2001;129:321–327.
13. Tome FM, Fardeau M. Congenital myopathy with "reducing bodies" in muscle fibres. Acta Neuropathol (Berl) 1975;31:207–217.
14. Watts GD, Wymer J, Kovach MJ, Mehta SG, Mumm S, Darvish D, et al. Inclusion body myopathy associated with Paget disease of bone and frontotemporal dementia is caused by mutant valosin-containing protein. Nat Genet 2004;36:377–381.

Available online at www.sciencedirect.com
ScienceDirect
Neuroscience Research 57 (2007) 513–521
Neuroscience Research
www.elsevier.com/locate/neures

Characterization of lobulated fibers in limb girdle muscular dystrophy type 2A by gene expression profiling

Yoko Keira [a,b], Satoru Noguchi [a], Rumi Kurokawa [a], Masako Fujita [a], Narihiro Minami [a], Yukiko K. Hayashi [a], Takashi Kato [b,c], Ichizo Nishino [a,*]

[a] *Department of Neuromuscular Research, National Institute of Neuroscience, National Center of Neurology and Psychiatry, 4-1-1 Ogawahigashi-cho, Kodaira, Tokyo 187-8502, Japan*
[b] *Graduate School of Science and Engineering, Waseda University, Tokyo, Japan*
[c] *Department of Biology, School of Education, Waseda University, Tokyo, Japan*

Received 13 September 2006; accepted 13 December 2006
Available online 5 January 2007

Abstract

Limb girdle muscular dystrophy type 2A (LGMD2A) is caused by mutations in *CAPN3*, which encodes an intracellular cysteine protease. To elucidate the fundamental molecular changes that may be responsible for the pathological features of LGMD2A, we employed cDNA microarray analysis. We divided LGMD2A muscles into two groups according to specific pathological features: an early-stage group characterized by the presence of active necrosis and a regeneration process and a later-stage group characterized by the presence of lobulated fibers. After comparing the gene expression profiles of the two groups of LGMD2A muscles with control muscles, we identified 29 genes whose mRNA expression profiles were specifically altered in muscles with lobulated fibers. Interestingly, this group included genes that encode actin filament binding and regulatory proteins, such as gelsolin, PDZ and LIM domain 3 (PDLIM3) and troponin I1. Western blot analysis confirmed the upregulation of these proteins. From these results, we propose that abnormal increased expression of actin filament binding proteins may contribute to the changes of the intramyofiber structures, observed in lobulated fibers in LGMD2A.

Keywords: Actin filament; Calpain 3; cDNA microarray; Limb girdle muscular dystrophy type 2A; Lobulated fiber; Myofibril

1. Introduction

Limb girdle muscular dystrophy (LGMD) is a group of disorders characterized by progressive atrophy and weakness of muscles in proximal limbs, scapular/pelvic girdle and trunk sparing facial muscles (Fardeau et al., 1996). At present, seven autosomal dominant and eleven autosomal recessive forms are known. LGMD2A is the most common form of LGMD and accounts for about 26% in Japan (Chae et al., 2001; Fanin et al., 2005). As with other muscular dystrophies, LGMD2A muscles show active necrotic and regenerating process in earlier stages of the disease. In later stages, however, the muscle pathology is characterized mainly by the presence of lobulated fibers (LF), which are composed of misaligned myofibrils that form a lobular pattern, in addition to fiber size variation and interstitial fibrosis (Guerard et al., 1985).

LGMD2A is caused by mutations in *CAPN3* encoding calpain 3, a skeletal muscle-specific non-lysosomal cysteine protease (Richard et al., 1995). Calpain 3 is present on myofibrils and specifically binds to the N2A and M line of titin, a muscle elastic protein (Sorimachi et al., 1995; Keira et al., 2003), although the *in vivo* substrate(s) of calpain 3 have not yet been well characterized. Most of the identified mutations in *CAPN3* are missense mutations, and are distributed throughout the exons of this gene.

LGMD2A is thought to be due to the loss of calpain 3 activity on myofibrils, nevertheless, the detailed pathomechanism remains to be elucidated. Interestingly, calpain 3 deficiency

Abbreviations: cDNA, complementary deoxyribonucleic acid; DMD, duchenne muscular dystrophy; ECM, extracellular matrix; GAPDH, glyceraldehyde phosphate dehydrogenase; H&E, hematoxylin and eosin staining; LGMD, limb girdle muscular dystrophy; LF, lobulated fiber; NADH-TR, β-nicotinamide adenine dinucleotide–tetrazolium reductase; NRF, necrotic and regenerating fiber; PDLIM3, PDZ and LIM domain 3; SPAG9, sperm-associated antigen 9; TUNEL, TdT-mediated dUTP-biotin nick end labeling

* Corresponding author. Tel.: +81 42 346 1712; fax: +81 42 346 1742.
E-mail address: nishino@ncnp.go.jp (I. Nishino).

0168-0102/$ – see front matter
doi:10.1016/j.neures.2006.12.010

has been shown to cause myonuclear apoptosis in association with subsarcolemmal localization and accumulation of NF-κB, resulting in perturbations in the IκBα/NF-κB pathway (Baghdiguian et al., 1999; Richard et al., 2000). However, this scenario probably cannot fully explain the pathomechanism of LGMD2A, especially the formation of LF in LGMD2A. To elucidate the pathomechanisms of LGMD2A, we obtained the comprehensive gene expression profiles using a muscle-specific cDNA microarray, and focused our attention on LF, which is a pathological hallmark of LGMD2A muscles in later stage.

2. Materials and methods

2.1. Patients

Muscle specimens from seven patients with genetically confirmed LGMD2A and two healthy controls (21 and 71 years old) were used in this study. A clinical summary of the patients is shown in Table 1. Except for patient 6, all of the patients with calpain 3 mutations were reported in our previous study (Chae et al., 2001). Patient 6 was genetically diagnosed by performing direct sequencing of PCR products amplified from cDNA and genomic DNA.

Genomic DNA analysis showed the presence of a homozygous (c.1524 + 1G > T) mutation, which resulted in the generation of an abnormal product (r.1426_1524del) through the activation of a cryptic splice site in exon 11. The biceps brachii muscle from each patient was biopsied after receiving informed consent and was immediately frozen in liquid nitrogen-cooled isopentane. We performed a battery of histochemical stainings on the biopsy, including hematoxylin and eosin (H&E) staining and β-nicotinamide adenine dinucleotide–tetrazolium reductase (NADH-TR) staining. Muscle samples were categorized into two groups according to their histological characteristics: a group with many necrotic and regenerating fibers (NRF in Fig. 1) and a group with LFs (LF in Fig. 1). Electron microscopic observation confirmed the presence of misaligned myofibrils and accumulation of mitochondria in the subsarcolemmal region, a typical feature of LF (Fig. 1F).

2.2. Gene expression profiling and data analysis

Customized cDNA microarray using 5760 probes for the 4200 genes expressed in human skeletal muscle were used in this study. A modified microarray technique allowing gene expression profiling to be performed even with a small amount of individual biopsied muscle was employed (Noguchi et al., 2003, 2005; Taniguchi et al., 2006). RNA extraction, hybridization, and detection of hybridized probes were done as previously described (Noguchi et al., 2003). Briefly, RNA was extracted from frozen muscles of LGMD2A patients and controls. We used a two-color labeling method in our microarray, because this method gives data with small variance, resulting in greater reproducibility and reliability than the one-colored method. In order to compare data between arrays, we performed competitive hybridization of each patient's RNA with a common RNA as one of probes. The relative expression values of this RNA were used to correct the hybridization efficiency in each array. The microarray was hybridized competitively with Cy3-labeled cDNA probes obtained from the RNA of each biopsied muscle, and Cy5-labeled cDNA probes from commercially available RNA (Origene, Rochville, MD, USA), which served as reference RNA for per-spot normalization. For each specimen, microarray experiments were carried out at least twice. Analysis of microarray data was performed using Genespring software 4.2.1 (Agilent, Palo Alto, CA, USA) and Microsoft Excel (Microsoft, Redmond, WA, USA). For per-spot normalization, the ratio of Cy3 to Cy5 intensity on each spot was used for the analyses. When the Cy5 intensity of a spot fell below 10.0, the data was not used. In addition, intensity-dependent (Lowess) normalization per chip was performed to minimize for variation in each microarray experiment. By combining repeated experiments, we identified single-fold changes and significance

Table 1
Clinical and molecular data of LGMD2A patient

Patient	Sex	Age at biopsy (years)	Disease duration (years)	Walking ability at biopsy (years)	Number of necrotic fibers in whole section	Regerating fibers (%)	Lobulated fibers (%)	TUNEL (%)	Calpain 3 gene mutation	Predicted protein change	Calpain 3 protein (%) (MWB[a])
1	F	7	Pre	No symptom	>2	>2	0	0.0056	c.1742C > G, c.2050 + 1G > A	p.S581C, p.(r.spl)	37.3
2	M	40	1	Defect of gait	>2	>2	0	0.014	c.2120A > G, c.1795dupA	p.D707G, p.T559fs	13.8
3	M	25	5	Difficulty of climbing stairs, Gowers sign	>5	>10	0	0	c.698G > T, c.2120A > G	p.G233V, p.D707G	4.9
4	M	56	21	Unable to walk without stick, Gowers sign	0	0	>60	n.t.[b]	c.2120A > G (homozygote)	p.D707G	0
5	M	27	15	Waddling gait, Gowers sign	<2	0	>30	0.0004	c.440G < C, c.?	p.R147P, p.0 (r.0)	0
6	M	32	17	Waddling gait, Gowers sign	0	0	>60	n.t.[b]	c.1524 +1G > T (homozygote)	p.V476_E508del[c]	0
7	M	49	11	Unable to climb stairs without banister	<2	<0.5	>60	0.008	C.1381C > T (homozygote)	p.R461C	43

[a] MWB: Multiplex Western Blotting.
[b] n.t.: Not tested.
[c] RT-PCR analysis showed an abberant splicing product (r.1426_1524del) in P6.

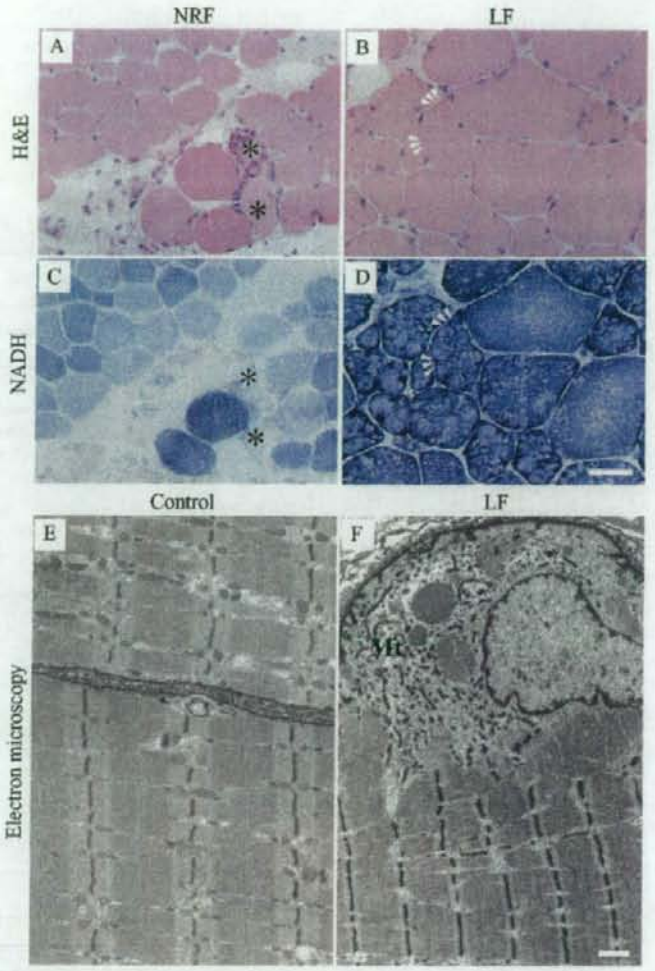

Fig. 1. Two representative muscle pathologies in LGMD2A. Microscopic images of hematoxylin and eosin (H&E) staining (A, B) and nicotinamide adenine dinucleotide tetrazolium reductase (NADH-TR) staining of LGMD2A patients (C, D). Patient 1 was classified into NRF group (A, C), and Patient 7 was classsified into LF group (B, D). Some necrotic (asterisks) and regenerative fibers were observed in the NRF patient and many lobulated fibers (arrowheads) were observed in the LF patient. Bar: 50 μm. Electronmicroscopic images of subsarcolemmal region in control (E) and LGMD2A patients with LF (F), respectively. Note accumulation of mitochondria (Mt) and disruption of myofibrils (F). Bar: 1 μm.

values for data points that were common to multiple microarrays. Hierarchical analyses were performed by using Pearson correlation (Fig. 2 and S1).

2.3. Quantitative RT-PCR

Quantitative RT-PCR was performed with QuantiTect SYBR Green PCR kit (Qiagen GmbH, Hilden, Germany) using iCycler iQ real-time PCR detection system (Bio-Rad, Hercules, CA, USA). We quantitated the amounts of gelsolin and glyceraldehyde phosphate dehydrogenase (GAPDH) transcripts as an internal control. Primer sequences used in this study are as follows. Gelsolin (forward: 5′-GACTTCTGCTAAGCGGTACATCGAG-3′, reverse: 5′-CACAAAGGAGGGAGGCTCAAAG-3′) and GAPDH (forward: 5′-GGTAAAGTGGATATTGTTGCCATCAATG-3′, reverse: 5′-GGAGGGATCTCGCTCCTGGAAGATGGTG-3′).

2.4. Western blotting

Cryosections of muscles were dissolved by heating them in 50 mM Tris–HCl, pH 6.8, 10% glycerol, 2% SDS, 2.5% 2-mercaptoethanol. Equal amounts of protein were separated by Laemmli SDS–PAGE in each lane of a 5–17.5% polyacrylamide gel and then transferred to polyvinyl-difluoride membranes. The membrane was then incubated with antibodies for gelsolin (1:2500 dilution; monoclonal) (clone No. 2, BD Bioscience, San Jose, CA, USA), PDZ and LIM domain 3 (PDLIM3) (1:5000 dilution; polyclonal) (Abcam, Cambridge, UK), and troponin I1 (1:5000 dilution; polyclonal) (Santa Cruz Biotechnology, Inc., Santa Cruz, CA, USA) at room temperature for 1 h. Subsequent incubation with peroxidase-conjugated goat anti-mouse IgG (H + L) (Immunotech, Beckman coulter, Germany), Histofine rabbit anti-goat IgG (Vector Lab. Burlingame, CA, USA) and peroxidase-conjugated goat anti-rabbit IgG (TAGO immunologicals, Camarillo, CA, USA) was performed at

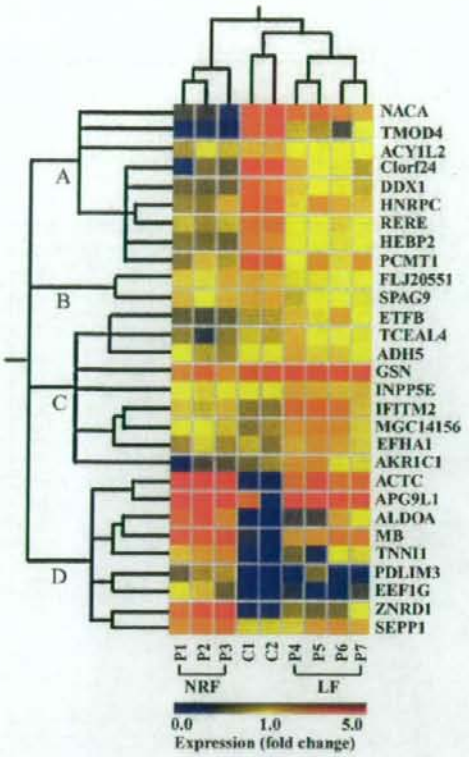

Fig. 2. Hierarchical analysis of the 29 selected genes according to their expression profiles. One block corresponds to one probe, which represents one gene. The expression of each gene relative to that of the reference RNA is shown in graduated colors as a scale to the right. Data for each subject are shown in vertical column in order to categorize the subjects into the NRF, control, or LF group. Color intensities among blocks in a row, which corresponds to a single gene, were compared. For cluster analysis, the 29 genes listed in the right dendrogram were subjected to Pearson correlation and were grouped as branches A–D, as shown on the left dendrogram. The color bar indicates the mRNA expression level of each muscle specimen as estimated from the signal ratio normalized with commercially Origene RNA. P: patient, C: control.

room temperature for 30 min. Membrane was developed using chemiluminescent reagent (Amersham Pharmacia Biotech UK, Buckinghamshire, UK).

2.5. Immunohistochemistry

Immunohistochemical staining was performed as described previously (Keira et al., 2003). We used the same gelsolin, troponin I1, and PDLIM3 antibodies as used in western blot analysis. Appropriate secondary antibodies used were affinity purified goat $(Fab)_2$ anti-rabbit IgG antibody conjugated with fluorescein (Tago, Inc., Burlingame, CA, USA), affinity purified goat anti-mouse IgG (H + L) antibody conjugated with fluorescein (Biosource International, Inc. Camarillo, CA, USA), and rabbit anti-goat IgG Alexa Fluor488 (Molecular probes, Inc., Eugene, OR, USA).

2.6. Apoptosis assay

The TdT-mediated dUTP-biotin nick end labeling (TUNEL) method was performed using an in situ apoptosis detection kit (Takara Co., Ltd., Japan) according to the manufacture's protocol. About 1000 myonuclei on different sections were counted and the percentages of TUNEL-positive myonuclei of each LGMD2A muscle were calculated.

3. Results

3.1. Overview of expression profiling in LGMD2A muscles

We analyzed the expression of more than 4200 genes in skeletal muscles of seven LGMD2A patients and two control individuals. Hierarchical analysis of all 4200 genes was performed to establish an association between the gene expression profile and the type of mutation in *CAPN3*, the residual amount of calpain 3 protein in muscle, and the muscle pathological findings (S1). We found that the pattern of gene expression was well delineated between the three groups, namely NRF, LF and controls. However, clustering analysis of non-selected genes gave results that were difficult to interpret. In order to elucidate the molecular events governing the formation of LFs, we performed further statistical analysis of the association between the expression profiles and the different muscle pathologies. Among the 4200 genes on the cDNA microarray, 207 genes were differentially expressed in LF muscles compared to control using the ANOVA–Welch *t*-test (statistically significant at $P < 0.01$) (S2 and S3). We classified these genes into 17 categories according to their functional characteristics. There were 150 upregulated genes and 57 downregulated genes in LF muscles (Table 2). Among the upregulated genes, genes associated with signal transduction, including calcium signalling-related genes, and cell growth-related genes predominated. In addition, ECM/membrane-related genes were also upregulated in LF muscles. On the other hand, genes related to energy metabolism comprised the majority of the downregulated genes. Similarly, by comparing LF and NRF muscles ($P < 0.01$), 423 genes were found to be differently expressed (S4 and S5). Among the 423 genes, 252 genes were upregulated, while 171 genes were downregulated in LF muscles (Table 3). Among the upregulated genes, the largest category was composed of transcription-related genes, while among downregulated genes, transport and sarcomere-related genes were predominant. Ubiquitin–proteasome-related genes, were also upregulated in LF muscles compared to other types of muscles. We also evaluated the changes in expression of genes related to apoptosis, since it has been reported that the apoptotic pathway is involved in the pathogenesis of LGMD2A (Baghdiguian et al., 1999). Among the 33 apoptosis-related genes in our microarray, eight genes (24%) showed altered expression in LGMD2A muscles (S2–S5). In summary, 207 genes were differentially expressed between LF and control muscles and 423 genes were differentially expressed between LF and NRF muscles. Further analysis revealed that 29 genes were common to both groups (Table 4). In addition, we performed ANOVA–Welch *t*-test with Bonferroni correction ($P < 0.05$) and found that nine genes were differentially expressed between all three groups (S6), although comparisons between NRF and the controls may not be so useful for understanding the pathomechanism of LF.

Table 2
Classification of differentially regulated 207 genes in LF muscles compared to normal muscles

Category	Number of genes with increased expression	Number of genes with decreased expression
Apoptosis	3	0
Catabolism	9	2
Channel/receptor	5	0
Chaperone	0	1
Cytoskeleton	10	3
ECM/membrane	15	0
Energy metabolism	14	8
Enzyme	6	1
Immune response	5	1
Lipid metabolism	3	0
Sarcomere	10	3
Signal transduction	18	7
Transcription	10	8
Translation	4	3
Transport	3	1
Others	13	5
Unknown	22	14
Total	150	57

Total 207 genes were differentially expressed in LF muscles compared to control using ANOVA–Welch *t*-test (statistically significant at $P < 0.01$). Gene categories are from LocusLink (www.ncbi.nlm.nih.gov/LocusLink).

3.2. Specifically dysregulated genes in LF muscles

We performed hierarchical clustering of the 29 genes using Pearson correlation. By experimental clustering, specimens were largely classified into three groups, which corresponded to NRF, LF and control as shown in the top dendrogram (Fig. 2).

Table 3
Classification of differentially regulated 423 genes in LF muscles compared to NRF muscles

Category	Number of genes with increased expression	Number of genes with decreased expression
Apoptosis	3	2
Catabolism	19	11
Channel/receptor	7	8
Chaperone	4	3
Cytoskeleton	8	3
ECM/membrane	8	5
Energy metabolism	16	12
Enzyme	5	4
Immune response	3	1
Lipid metabolism	3	2
Sarcomere	2	7
Signal transduction	30	28
Transcription	42	16
Translation	14	7
Transport	0	9
Others	32	13
Unknown	56	40
Total	252	171

Total 423 genes were differentially expressed in LF muscles compared to NRF muscles using ANOVA–Welch *t*-test (statistically significant at $P < 0.01$). Gene categories are from LocusLink (www.ncbi.nlm.nih.gov/LocusLink).

By hierarchical gene clustering, these 29 genes were divided into four branches (branches A–D) (Fig. 2 and Table 4). The genes in branch A were less downregulated in NRF and LF muscles than in the controls, albeit more downregulation was observed in the LF muscles. Branch A was predominantly comprised of transcription-related and RNA-binding protein genes, such as *HNRPC*, *DDX1* and *RERE*, and a gene (*TMOD4*) that encodes an actin regulatory protein, tropomodulin 4. Only two genes, including sperm-associated antigen 9 (*SPAG9*), were found in branch B. Genes in this branch were only mildly downregulated in LF muscles and nearly normally expressed in NRF muscles. The genes in branch C were upregulated in LF muscles but mildly downregulated or normal expressed in NRF muscles. Genes encoding signal-mediating molecules comprised the bulk of this group. Interestingly, of the nine genes in branch C, the expression of *GSN* gene, which encodes gelsolin, an actin depolymerizing or stabilizing plus end protein, was greatly increased about 11-fold in LF muscles compared to NRF muscles (Table 4). The genes in branch D were highly upregulated in NRF muscles and, to a lesser extent, in LF muscles, and primarily included genes that encode sarcomeric proteins such as *TNNI1*, *PDLIM3* and *ACTC*. Based on our previously reported data (Noguchi et al., 2003), the expression of five of the nine genes in branch D was also altered in DMD (Table 4).

3.3. Changes in the expression of actin-associated genes in LF muscles

Of the 29 selected genes, we further focused on the upregulated genes *GSN*, *TNNI1* and *PDLIM3*, which encode

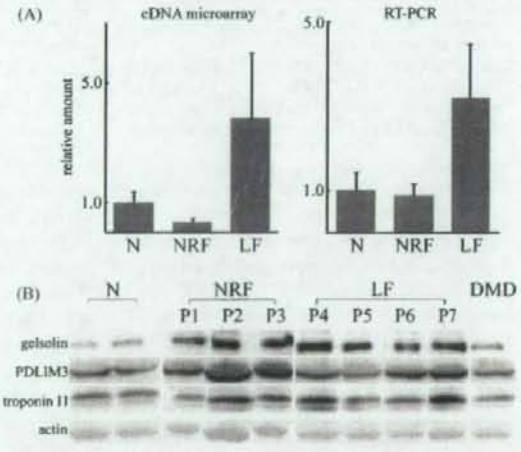

Fig. 3. Validation of cDNA microarray data by quantitative RT-PCR and Western blot analysis. Measurements of mRNA expression of *GSN* using cDNA array analysis or quantitative RT-PCR analysis (A). Western blot analysis of gelsolin, PDLIM3 and troponin I1 using skeletal muscle homogenates from seven LGMD2A patients, two controls, and one DMD patient (B). Note that compared to controls, the expression of these three proteins increases in both NRF and LF patients. The actin band was stained with Coomasie brilliant blue as a control.

Table 4
Specifically regulated 29 genes in patients with lobulated fibers

Accession	Gene	Function	LF/N	LF/NR	DMD	LGMD2B
(A)						
NM_022083	Clorf24	Unknown	−5.7	1.8		
NM_013353	TMOD4	Muscle structure	−4.6	2.6	Down[a]	
NM_005389	PCMT1	Chaperone	−2.8	1.6		
NM_004939	DDX1	Transcription	−2.7	1.5		
NM_031314	HNRPC	Transcription	−2.5	1.4		
NM_012102	RERE	Transcription	−2.1	1.2		
NM_005594	NACA	Others	−2.0	4.3		
NM_014320	HEBP2	Others	−1.8	1.4		
NM_001010853	ACY1L2	Catabolism	−1.1	1.2		
(B)						
NM_003971	SPAG9	Signal transduction	−1.4	−1.2		
NM_017875	FLJ20551	Others	−1.3	−1.2		
(C)						
NM_000177	GSN	Cytoskeletal protein	3.6	10.7	Up[a]	Up[b]
NM_006435	IFITM2	Immune response	3.0	2.0		
NM_032906	MGC14156	Signal transduction	2.0	1.6		
NM_001353	AKR1C1	Catabolism	1.6	2.6	Down[a]	
NM_152726	EFHA1	Signal transduction	1.6	1.6		
NM_001985	ETFB	Lipid metabolism	1.4	1.9	Down[a]	
NM_024863	TCEAL4	Translation	1.3	1.6		
NM_000671	ADH5	Redox	1.2	1.3		
AI026701	INPP5E	Signal transduction	1.2	1.1		
(D)						
NM_005159	ACTC	Muscle structure	14.4	−3.8	Up[a,c,d]	
NM_005368	MB	Energy metabolism	5.7	−2.1		
NM_024085	APG9L1	Catabolism	5.2	−2.1		
NM_014476	PDLIM3	Muscle structure	4.2	−2.1	Down[a]	
NM_000034	ALDOA	Glycolysis	3.9	−3.6	Down[a]	
NM_001404	EEF1G	Translation	3.7	−2.4	Down[a]	
NM_003281	TNNI1	Muscle structure	2.7	−1.9	Down[a]	
NM_170783	ZNRD1	Transcription	2.1	−5.0		
NM_005410	SEPP1	Extracellular matrix	1.5	−1.4		

LF/N represents the fold change in expression in muscles with LF to that in controls. LF/NR represents the fold change in expression in muscles with LF to that with NRF. (−) Denotes down-regulation.

[a]Genes differentially regulated in DMD patients according to Noguchi et al. (2003, 2005).
[b]Genes differentially regulated in LGMD2B patients according to Campanaro et al. (2002).
[c]Genes differentially regulated in DMD patients according to Chen et al. (2000).
[d]Genes differentially regulated in DMD patients according to Haslett et al. (2002).

cytoskeletal and sarcomeric proteins, because myofibrillar structure is greatly altered in LF muscles. We confirmed the upregulation of the *GSN* gene by quantitative RT-PCR (Fig. 3A) and the increase in the expression of its product, gelsolin, by Western blotting (Fig. 3B). Quantitative RT-PCR analysis showed four-fold upregulation of this gene in LF muscles as compared with NRF muscles (Fig. 3A). Moreover, protein expression of gelsolin was increased about 10-fold in LGMD2A muscles when compared with the control. However, there was no difference between LF muscles and NRF muscles (Fig. 3B). Immunohistochemical analysis of LF muscles showed that gelsolin was distributed in the subsarcolemmal regions of LFs (Fig. 4, patient 6, asterisks), and in connective tissue, although it was undetectable in control muscle fibers. In addition, in NRF muscles, gelsolin was diffusely present in the cytoplasm of small regenerating fibers and in the subsarcolemmal region of necrotic fibers and mononuclear cells (Fig. 4).

We also confirmed the upregulation of PDLIM3 and troponin I1 proteins by Western blot analysis both in NRF and LF muscles (Fig. 3B). Immunohistochemistry showed that the sarcomere of LFs and non-LFs was strongly stained with PDLIM3. In contrast, in NRF muscles, immunoreactivity was only mildly increased in apparently unaffected muscle fibers (Fig. 4). Troponin I1 expression was increased in the sarcomere of the small LFs. Fiber typing by anti-myosin heavy chain antibody showed that most of these small muscle fibers were slow-type fibers (data not shown, Chae et al., 2001). In NRF muscles, however, signals were undetectable in either necrotic or regenerating fibers (Fig. 4).

4. Discussion

In our analysis, we have clearly shown that gene expression in LGMD2A can be classified on the basis of differences in muscle pathology (S1), as with other muscular dystrophies

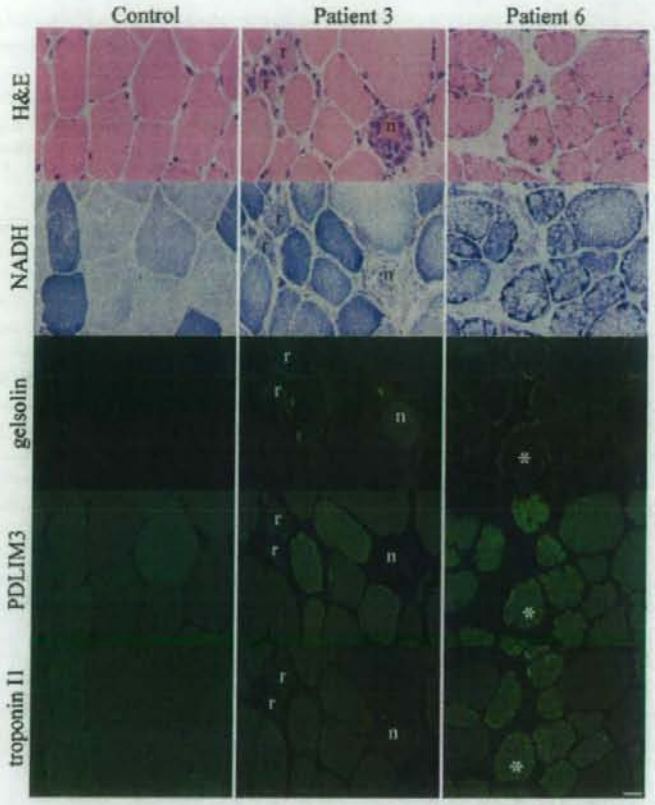

Fig. 4. Immunohistochemical analyses of gelsolin, PDLIM3 and troponin I1 reveal abnormal staining in NRF and LF muscles. Gelsolin, PDLIM3 and troponin I1were stained in control, NRF muscle (Patient 3) and LF muscle (Patient 6). Gelsolin localizes in the cytoplasmic region of regenerating fiber (r) and peripheral region of necrotic fiber (n), and the subsarcolemmal region of LFs (asterisk) and connective tissues. PDLIM3 showed a striation pattern in the control; however, it was not detectable in regenerating (r) or necrotic fibers (n) in NRF muscles (Patient 3). In LF muscle, PDLIM3 is abundantly distributed in the sarcomeric region of LFs (asterisks, Patient 6). Troponin I1 displayed diffuse sarcomeric staining in slow-type fibers in control and NRF muscles (Patient 3), and it localized strongly to the sarcomeric region of many slow-type LFs (white asterisk). Bar: 20 μm.

(Noguchi et al., 2003; Taniguchi et al., 2006). This suggests that the pathological changes seen in LGMD2A muscles might well be caused by molecular events initiated by these differences in gene expression. Since LF is characteristically observed in the later stage of LGMD2A, we therefore divided LGMD2A patients into two groups on the basis of pathological features in order to uncover the characteristic gene expression profiles of LGMD2A.

4.1. Outline of expression profiles in LF muscles

In LF muscles, several genes related to signal transduction and transcription were differentially expressed. These genes encode signaling mediators and transcriptional factors implicated in cell growth, calcium signaling and apoptosis. Interestingly, our results suggested that the genes for cell growth and calcium signaling were upregulated; in contrast, genes involved in apoptosis were rather suppressed in LF muscles. These data suggested that apoptosis signaling might be inactivated at least in LF or the later stage of LGMD2A muscles. In fact, the ratio of TUNEL-positive myonuclei to normal nuclei was less than 0.014% in our series (Table 1).

Genes coding for extracellular matrix (ECM)/membrane-related, cytoskeletal or sarcomeric proteins were also upregulated in LF muscles. These molecular changes could reflect the structural features of LF muscles. For example, upregulation of ECM/membrane-related genes might be associated with interstitial fibrosis observed in LF muscles; likewise, upregulation of cytoskeletal or sarcomeric-related genes might be associated with structural changes of the intramyofibril network in LFs.

The expression changes of some genes in the NRF muscles of LGMD2A patients were similar to those seen in Duchenne muscular dystrophy (DMD) muscles. In our previous study, in muscles from DMD patients, upregulated genes were mostly those related to immune response, sarcomeric, ECM and signal transduction, whereas, downregulated genes were associated with energy metabolism, transcription/translation,

signal transduction and the proteasome (Noguchi et al., 2003). In the present study, however the expression levels of these genes in LF stage were similar to those in control muscles. These results confirm the absence of necrotic and regenerating processes in LF muscles.

4.2. The 29 specifically dysregulated genes in LF muscles

4.2.1. Overview of the 29 genes in LF muscles

As shown in Table 4, we found that the expression of the genes in branch A was comparable between control and LF but was greatly decreased in NRF muscles. On the other hand, the expression of genes in branch D was greatly increased in NRF muscles compared to LF muscles. From these results, we considered that the expression of genes in branches A and D might be closely related to necrosis and regeneration in NRF. In contrast, the expression of genes in branches B and C underwent more extensive downregulation or upregulation in LF than in NRF. The genes in these branches may play specific roles in LF formation, although we were unable to get any conclusive information about, or identify common properties between the genes in these groups.

4.2.2. Apoptosis-associated genes among the 29 genes

Among the 29 genes, genes related to cytoskeletal, sarcomeric, signal transduction and catabolism proteins were upregulated, while genes related to transcription were downregulated in LF muscles. One of the downregulated genes was *SPAG9*, which encodes a scaffold protein that binds to several signaling molecules or transcription factors (Lee et al., 2002). Interestingly, SPAG9 interacts with NF-κB1/p105 but not with NF-κB2/p100, and expression of RNAi for *SPAG9* results in decreased NF-κB activity in response to treatment with tumor necrosis factor-α (Bouwmeester et al., 2004). NF-κB signaling pathway was reported to be downregulated in muscles from LGMD2A patients and calpain 3 knockout mice (Baghdiguian et al., 1999; Richard et al., 2000). The down-regulation of *SPAG9* observed in this study may partly reflect perturbation of the NF-κB signaling pathway as reported by Baghdiguian. Although, as earlier mentioned, other apoptotic signals seemed to be suppressed in LF, a more extensive analysis of the NF-κB pathway in LGMD2A patients is still needed to clarify the role of SPAG9 and other related genes in apoptosis.

4.2.3. Actin-associated genes among the 29 genes

Since the presence of LF is a characteristic structural change observed in LGMD2A muscles, changes in the expression of genes encoding intracellular structural proteins and their regulators should be important. In this study, we focused on upregulated genes for actin-associated proteins in LF muscles, such as gelsolin, troponin I1 and PDLIM3.

4.2.3.1. Gelsolin. A comparison of the present data with our previous data (Noguchi et al., 2003) shows that gelsolin gene expression is more upregulated in LF than in DMD muscles. We found that gelsolin was distributed diffusely in the cytoplasm of regenerating fibers, in contrast to its subsarcolemmal distribution in LFs, which are characterized by deranged myofibrils and mitochondria accumulation. Gelsolin mainly functions to sever actin filament and to cap the plus ends of the severed filaments (Yin et al., 1981; Lamb et al., 1993). In cultured myogenic cells, myofibrils develop resistance to this severing function of gelsolin during differentiation (Huckriede et al., 1988; Gonsior and Hinssen, 1995). Taking all the available information into account, we consider the following roles for gelsolin during its activation in LF:1) gelsolin could scavenge the disrupted actin-containing thin filaments of LFs and 2) gelsolin could sever the subsarcolemmal cytoskeletal actin network. Although we have no supportive evidence for any of these possibilities, the upregulation of gelsolin may be associated with actin derangement in LFs.

4.2.3.2. TroponinI1. Troponin I is a subunit of the actin filament-associated troponin–tropomyosin complex involved in the regulation of skeletal and cardiac muscle contraction (Gordon et al., 2000). In our study, troponin I1, which is a slow-twitch isoform of troponin I family, was highly upregulated in LGMD2A muscles with NRF, and to a lesser extent, in those with LF (Table 4). Other subunit genes in the troponin complex, such as *TNNI2*, *TNNC1*, *TNNC2* and *TNNT3* were also strongly upregulated in LGMD2A muscles with NRF and weakly in those with LF (S1). Expression of each troponin subunit gene seems to be similarly regulated during the progression of muscle pathology in LGMD2A. In LF muscles, troponin I1 immunoreactivity was observed strongly in the small slow-type LFs. Considering the predominance of slow-twitch fibers in LF muscles, the increase in troponin I1 mRNA expression in LF muscles might be due to the increased numbers of slow fibers in LF muscles (Chae et al., 2001). Interestingly, troponin I1 was not observed in the subsarcolemmal region and did not co-localize with gelsolin in LFs. From this result, the intensive expression of troponin I1 might not be directly related to the derangement of myofibrils in subsarcolemmal regions in LFs.

4.2.3.3. PDLIM3. PDLIM3 is known to bind the spectrin-like repeats of α-actinin via its PDZ domain and localize to the Z-lines (Xia et al., 1997; Jo et al., 2001). It has been reported that overexpression of PDLIM3 results in the increased ability of α-actinin to cross-link actin filaments (Pashmforoush et al., 2001). In our study, PDLIM3 showed stronger immunoreactivity in LFs, but did not colocalize with gelsolin accumulation. The upregulation of PDLIM3 observed in LF muscles might have some roles in stabilizing Z-line of myofibril structures.

4.3. Conclusion

Upregulation of the genes associated with actin filament observed in LF muscles is consistent with the markedly disorganized myofibrils in these muscles. Although, further analyses will be needed to explain relationship between calpain 3 and associated molecules whose functions remain unknown, our study shows that gene expression profiling of LGMD2A is a powerful tool that can provide clues to the pathomechanism of this disease.

Acknowledgments

The authors thank Drs. I. Nonaka, M. Malicdan and M. Astejada (National Center of Neurology and Psychiatry) for helpful discussions and their critical comments on the manuscript, and Ms. F. Uematsu for her technical assistance. This study was supported by the "Research on Psychiatric and Neurological Diseases and Mental Health" from Health and Labour Sciences Research Grants; the "Research on Health Sciences focusing on Drug Innovation" from the Japanese Health Sciences Foundation; the "Research Grant (16B-2, 17A-10) for Nervous and Mental Disorders" from the Ministry of Health, Labour and Welfare; and the Program for Promotion of Fundamental Studies in Health Sciences of the National Institute of Biomedical Innovation (NIBIO).

Appendix A. Supplementary data

Supplementary data associated with this article can be found, in the online version, at doi:10.1016/j.neures.2006.12.010.

References

Baghdiguian, S., Martin, M., Richard, I., Pons, F., Astier, C., Bourg, N., Hay, R.T., Chemaly, R., Halaby, G., Loiselet, J., Anderson, L.V., Lopez de Munain, A., Fardeau, M., Mangeat, P., Beckmann, J.S., Lefranc, G., 1999. Calpain 3 deficiency is associated with myonuclear apoptosis and profound perturbation of the IkappaB alpha/NF-kappaB pathway in limb-girdle muscular dystrophy type 2A. Nat. Med. 5, 503–511.

Bouwmeester, T., Bauch, A., Ruffner, H., Angrand, P.O., Bergamini, G., Croughton, K., Cruciat, C., Eberhard, D., Gagneur, J., Ghidelli, S., Hopf, C., Huhse, B., Mangano, R., Michon, A.M., Schirle, M., Schlegl, J., Schwab, M., Stein, M.A., Bauer, A., Casari, G., Drewes, G., Gavin, A.C., Jackson, D.B., Joberty, G., Neubauer, G., Rick, J., Kuster, B., Superti-Furga, G., 2004. A physical and functional map of the human TNF-alpha/NF-kappa B signal transduction pathway. Nat. Cell Biol. 6, 97–105.

Campanaro, S., Romualdi, C., Fanin, M., Celegato, B., Pacchioni, B., Trevisan, S., Laveder, P., De Pitta, C., Pegoraro, E., Hayashi, Y.K., Valle, G., Angelini, C., Lanfranchi, G., 2002. Gene expression profiling in dysferlinopathies using a dedicated muscle microarray. Hum. Mol. Genet. 11, 3283–3298.

Chae, J., Minami, N., Jin, Y., Nakagawa, M., Murayama, K., Igarashi, F., Nonaka, I., 2001. Calpain 3 gene mutations: genetic and clinico-pathologic findings in limb-girdle muscular dystrophy. Neuromuscul. Disord. 11, 547–555.

Chen, Y.W., Zhao, P., Borup, R., Hoffman, E.P., 2000. Expression profiling in the muscular dystrophies: identification of novel aspects of molecular pathophysiology. J. Cell Biol. 151, 1321–1336.

Fanin, M., Nascimbeni, A.C., Fulizio, L., Angelini, C., 2005. The frequency of limb girdle muscular dystrophy 2A in northeastern Italy. Neuromuscul. Disord. 15, 218–224.

Fardeau, M., Hillaire, D., Mignard, C., Feingold, N., Feingold, J., Mignard, D., de Ubeda, B., Collin, H., Tome, F.M., Richard, I., Beckmann, J.S., 1996. Juvenile limb-girdle muscular dystrophy. Clinical, histopathological and genetic data from a small community living in the Reunion Island. Brain 119, 295–308.

Gonsior, S., Hinssen, H., 1995. Exogenous gelsolin binds to sarcomeric thin filaments without severing. Cell Motil. Cytoskeleton 31, 196–206.

Gordon, A.M., Homsher, E., Regnier, M., 2000. Regulation of contraction in striated muscle. Physiol. Rev. 80, 853–924.

Guerard, M.J., Sewry, C.A., Dubowitz, V., 1985. Lobulated fibers in neuromuscular desease. J. Neurol. Sci. 69, 345–356.

Haslett, J.N., Sanoudou, D., Kho, A.T., Bennett, R.R., Greenberg, S.A., Kohane, I.S., Beggs, A.H., Kunkel, L.M., 2002. Gene expression comparison of biopsies from Duchenne muscular dystrophy (DMD) and normal skeletal muscle. Proc. Natl. Acad. Sci. USA 99, 15000–15005.

Huckriede, A., Hinssen, H., Jockusch, B.M., Lazarides, E., 1988. Gelsolin sensitivity of microfilaments as a marker for muscle differentiation. Eur. J. Cell Biol. 46, 506–512.

Jo, K., Rutten, B., Bunn, R.C., Bredt, D.S., 2001. Actinin-associated LIM protein-deficient mice maintain normal development and structure of skeletal muscle. Mol. Cell Biol. 21, 1682–1687.

Keira, Y., Noguchi, S., Minami, N., Hayashi, Y.K., Nishino, I., 2003. Localization of calpain 3 in human skeletal muscle and its alteration in limb-girdle muscular dystrophy 2A muscle. J. Biochem. (Tokyo) 133, 659–664.

Lamb, J.A., Allen, P.G., Tuan, B.Y., Janmey, P.A., 1993. Modulation of gelsolin function. Activation at low pH overrides Ca^{2+} requirement. J. Biol. Chem. 268, 8999–9004.

Lee, C.M., Onesime, D., Reddy, C.D., Dhanasekaran, N., Reddy, E.P., 2002. JLP: a scaffolding protein that tethers JNK/p38MAPK signaling modules and transcription factors. Proc. Natl. Acad. Sci. USA 99, 14189–14194.

Noguchi, S., Tsukahara, T., Fujita, M., Kurokawa, R., Tachikawa, M., Toda, T., Tsujimoto, A., Arahata, K., Nishino, I., 2003. cDNA microarray analysis of individual Duchenne muscular dystrophy patients. Hum. Mol. Genet. 12, 595–600.

Noguchi, S., Fujita, M., Murayama, K., Kurokawa, R., Nishino, I., 2005. Gene expression analyses in X-linked myotubular myopathy. Neurology 65, 732–737.

Pashmforoush, M., Pomies, P., Peterson, K.L., Kubalak, S., Ross Jr., J., Hefti, A., Aebi, U., Beckerle, M.C., Chien, K.R., 2001. Adult mice deficient in actinin-associated LIM-domain protein reveal a developmental pathway for right ventricular cardiomyopathy. Nat. Med. 7, 591–597.

Richard, I., Broux, O., Allamand, V., Fougerousse, F., Chiannilkulchai, N., Bourg, N., Brenguier, L., Devaud, C., Pasturaud, P., Roudaut, C., Hillaire, D., Passos-Bueno, M.R., Zatz, M., Tischfield, A.J., Fardeau, M., Jackson, E.C., Cohen, D., Beckmann, J.S., 1995. Mutations in the proteolytic enzyme calpain 3 cause limb-girdle muscular dystrophy type 2A. Cell 81, 27–40.

Richard, I., Roudaut, C., Marchand, S., Baghdiguian, S., Herasse, M., Stockholm, D., Ono, Y., Suel, L., Bourg, N., Sorimachi, H., Lefranc, G., Fardeau, M., Sebille, A., Beckmann, J.S., 2000. Loss of calpain 3 proteolytic activity leads to muscular dystrophy and to apoptosis-associated IkappaBalpha/nuclear factor kappaB pathway perturbation in mice. J. Cell Biol. 151, 1583–1590.

Sorimachi, H., Kinbara, K., Kimura, S., Takahashi, M., Ishiura, S., Sasagawa, N., Sorimachi, N., Shimada, H., Tagawa, K., Maruyama, K., Suzuki, K., 1995. Muscle-specific calpain, p94, responsible for limb girdle muscular dystrophy type 2A, associates with connectin through IS2, a p94-specific sequence. J. Biol. Chem. 270, 31158–31162.

Taniguchi, M., Kurahashi, H., Noguchi, S., Fukudome, T., Okinaga, T., Tsukahara, T., Tajima, Y., Ozono, K., Nishino, I., Nonaka, I., Toda, T., 2006. Aberrant neuromuscular junctions and delayed terminal muscle fiber maturation in alpha-dystroglycanopathies. Hum. Mol. Genet. 15, 1279–1289.

Xia, H., Winokur, S.T., Kuo, W.L., Altherr, M.R., Bredt, D.S., 1997. Actinin-associated LIM protein: identification of a domain interaction between PDZ and spectrin-like repeat motifs. J. Cell. Biol. 139, 507–515.

Yin, H.L., Hartwig, J.H., Maruyama, K., Stossel, T.P., 1981. Ca^{2+} control of actin filament length. Effects of macrophage gelsolin on actin polymerisation. J. Biol. Chem. 256, 9693–9697.

OBSERVATION

Limb-Girdle Muscular Dystrophy Due to Emerin Gene Mutations

Shigehisa Ura, MD; Yukiko K. Hayashi, MD, PhD; Kanako Goto, MS; Mina Nolasco Astejada, MD; Terumi Murakami, MD; Masako Nagato, MD; Shigeru Ohta, MD; Yasuhisa Daimon, MD; Hidehiro Takekawa, MD, PhD; Koichi Hirata, MD, PhD; Ikuya Nonaka, MD, PhD; Satoru Noguchi, PhD; Ichizo Nishino, MD, PhD

Background: Emery-Dreifuss muscular dystrophy, caused by *EMD* gene mutations, is characterized by humeroperoneal muscular dystrophy, joint contractures, and conduction defects and is often associated with sudden cardiac death, even without prior cardiac symptoms.

Objective: To describe the clinical and molecular features of 2 patients with limb-girdle muscular dystrophy with mutations in *EMD*.

Design: Case reports.

Setting: Academic research.

Patients: Two male patients manifested proximal dominant muscle involvement, with minimal or no joint and cardiac involvement.

Main Outcome Measures: Muscle biopsy and mutation analysis results.

Results: Immunohistochemistry revealed an absence of emerin staining in muscle biopsy specimens. Mutation analysis identified nonsense mutations in *EMD*.

Conclusions: Mutations in *EMD* may indicate a limb-girdle muscular dystrophy phenotype. Identification of emerin deficiency among patients with limb-girdle muscular dystrophy is essential to prevent cardiac catastrophe.

Arch Neurol. 2007;64(7):1038-1041

Author Affiliations:
Department of Neuromuscular Research, National Institute of Neuroscience, National Center of Neurology and Psychiatry, Tokyo (Drs Ura, Hayashi, Astejada, Murakami, Nonaka, Noguchi, and Nishino and Ms Goto); Department of Pediatrics, Tenri Hospital, Nara (Drs Nagato and Ohta); and Department of Neurology, Dokkyo Medical University, Tochigi (Drs Daimon, Takekawa, and Hirata), Japan.

EMERY-DREIFUSS MUSCULAR dystrophy (EDMD) is a rare muscular dystrophy clinically characterized as a triad of (1) slowly progressive humeroperoneal muscular dystrophy; (2) early joint contractures of Achilles tendons, elbows, and hind neck; and (3) cardiomyopathy with conduction defects.[1] The X-linked form of EDMD is caused by mutations in the emerin gene (*EMD*) or in *STA* on Xq28,[2] whereas autosomal dominant and rare recessive forms of EDMD are caused by mutations in the lamin A/C gene (*LMNA*) on 1q21.[3] *EMD* is composed of 6 small exons that encode emerin, a 34-kDa inner nuclear membrane protein.[2,4] Immunohistochemical analysis is valuable for the diagnosis of the X-linked form of EDMD because most patients show a lack of emerin staining at the nuclear membrane of skin, leukocytes, and skeletal and cardiac muscles.[5-7] *LMNA* encodes lamin A and C, which are major components of nuclear lamina. Emerin and lamin A/C are nuclear envelope proteins, and clinical features of the X-linked form of EDMD and autosomal dominant EDMD are similar and indistinguishable. However, mutations in *LMNA* are known to be associated with several other disorders collectively known as *laminopathies*, including limb-girdle muscular dystrophy (LGMD) type 1B, which is characterized by proximal dominant muscular dystrophy with atrioventricular conduction disturbance.[8] To exclude *EMD* mutations in patients with LGMD, we examined emerin expression in muscle biopsy specimens and performed genetic screening.

METHODS

MUSCLE BIOPSY SPECIMENS

All clinical materials used in this study were obtained for diagnostic purposes following informed consent. Skeletal muscle biopsy specimens were flash frozen in isopentane chilled with liquid nitrogen. A panel of histochemical staining, including hematoxylin-eosin and modified Gomori trichrome, was performed to obtain the pathological diagnosis. Immunohistochemical and immunoblotting analyses

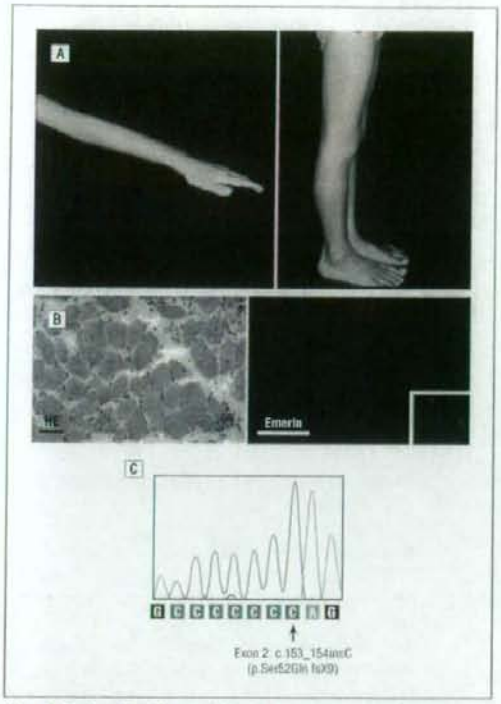

Figure 1. Patient 1. A, A 9-year-old boy had proximal muscle atrophy without joint contractures. B, Hematoxylin-eosin (HE) staining and emerin immunoreaction (Emerin) of skeletal muscle biopsy specimen. The HE staining shows fiber-size variation, regenerating fibers, and fibers with internalized nuclei. Immunoreaction of emerin is absent at the nuclear membrane. The bar indicates 50 μm. Inset, Emerin staining of control muscle is shown. C, Mutation analysis revealed a 1–base pair insertion at c.154 in exon 2.

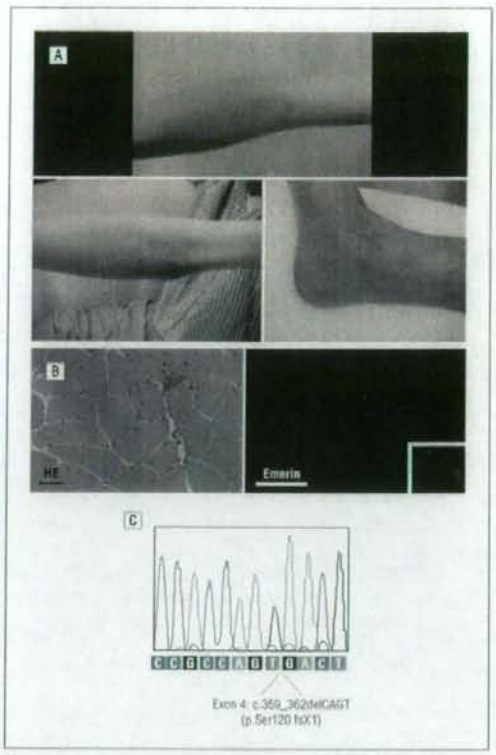

Figure 2. Patient 2. A, A 50-year-old man had proximal dominant muscle atrophy of the limbs with minimal joint contractures at the right elbow and Achilles tendon. B, Hematoxylin-eosin (HE) staining and emerin immunoreaction (Emerin) of muscle biopsy specimen. The HE staining shows fiber-size variation, regenerating fibers, and fibers with internalized nuclei. Immunoreaction of emerin is absent at the nuclear membrane. The bar indicates 50 μm. Inset, Emerin staining of control muscle is shown. C, Direct sequence analysis revealed a 4–base pair deletion at c.359-362 in exon 4.

were conducted as previously described.[9] Genomic DNA was extracted from muscle biopsy specimens or from peripheral lymphocytes using standard techniques.

We examined 94 patients who were clinically and pathologically diagnosed as having LGMD. Exclusion of LGMD types 1C, 2A to 2G, 2I, and 2K was performed by immunohistochemical and Western blotting analyses. In detecting emerin in skeletal muscle biopsy specimens, monoclonal antiemerin antibody (Novocastra Laboratories, New Castle upon Tyne, England) was used.

MUTATION ANALYSIS

All 6 exons and their flanking intronic regions of *EMD* were directly sequenced using an automated sequencer (ABI PRISM 3100; PE Applied Biosystems, Foster City, California). Information about the primers used for the sequence analysis is available from the corresponding author. Sequence analysis of *LMNA* was also performed to exclude LGMD type 1B.

RESULTS

Among 94 patients with LGMD of unknown cause, we identified 2 patients with negative immunostaining for emerin in their skeletal muscles (**Figure 1** and **Figure 2**). Mutation analysis of *EMD* revealed a 1–base pair (bp) insertion (c.153_154insC in exon 2) in patient 1 (Figure 1) and a 4-bp deletion (c.359_362delCAGT in exon 4) in patient 2 (Figure 2). Both mutations were predicted to cause premature termination codon and absence of protein expression.

REPORT OF CASES

Patient 1, a 9-year-old boy from nonconsanguineous parents, neither of whom had neuromuscular or cardiac disorders, was initially seen with proximal dominant muscle weakness and atrophy. He had normal developmental milestones, acquiring independent ambulation at age 1 year; however, unsteady gait was noticed at age 4 years. By age 6 years, he developed weakness and atrophy of the proximal muscles of the lower limbs, waddling gait, and lordotic posture. He then needed support in climbing stairs. On physical examination at age 6 years, his calf muscles were not atrophic. Serum creatine kinase levels were elevated to 927 U/L (to convert

to microkatal per liter, multiply by 0.0167) (reference range, <180 U/L). Muscle biopsy was performed on the left biceps brachii, and the biopsy specimen showed moderate fiber size variation, with some regenerating fibers and several fibers with internalized nuclei (Figure 1). Results of dystrophin immunostaining were positive, and he was diagnosed as having LGMD. At age 9 years, he showed Gowers sign, waddling gait, and proximal dominant limb muscle weakness and atrophy. No joint contractures were observed (Figure 1). An electrocardiogram revealed transient sinus arrhythmia, but his echocardiogram was normal.

Patient 2, a 50-year-old man, initially was seen with proximal dominant muscle weakness and atrophy. His father had died of acute myocardial infarction; his mother was alive without symptoms of neuromuscular or cardiac disorders. He was healthy until age 35 years, when he noticed difficulty in going up and down stairs. During this time, he was incidentally found to have hypertension. Muscle weakness was progressive, and he had difficulty raising his arms by age 40 years. At age 49 years, he required support in climbing stairs and had difficulty in buttoning his clothes. Although his electrocardiogram was normal, an echocardiogram demonstrated moderate mitral and tricuspid insufficiency without dilatation of ventricles. Other than his father's death from acute myocardial infarction, his family history was noncontributory. On physical examination, he had waddling gait, Gowers sign, and proximal dominant muscle weakness and atrophy. Only minimal joint contractures of the right elbow, bilateral Achilles tendons, and neck were observed (Figure 2). His serum creatine kinase level was elevated at 417 U/L. An electromyogram showed myopathy. Results of muscle computed tomography revealed proximal dominant muscle atrophy with fatty tissue replacement. A second electrocardiogram demonstrated complete atrioventricular conduction block. A muscle biopsy specimen was obtained from the left rectus femoris and showed marked fiber size variation, scattered regenerating fibers, and fibers with centrally placed nuclei (Figure 2).

COMMENT

Herein, we demonstrate an expanded clinical spectrum associated with *EMD* mutations, from the X-linked EDMD phenotype to the X-linked LGMD phenotype. The differences between EDMD and LGMD relate to the distribution of affected muscles and to the presence of early joint contractures. From childhood, patients with EDMD having an *EMD* or *LMNA* mutation may demonstrate slowly progressive weakness and wasting of humeroperoneal muscles. Early contracture of the elbows, Achilles tendons, and posterior cervical muscles is another characteristic cardinal feature. Mutations in *LMNA* are associated with variable disorders, including EDMD, LGMD type 1B, peripheral neuropathy, progelia syndromes, lipodystrophy syndrome, and cardiomyopathy with conduction defects. Several overlapping clinical conditions are likewise observed, including an intermediate phenotype of EDMD and LGMD type 1B manifesting as proximal limb muscle involvement with early joint contractures. In contrast, mutations in *EMD* have been associated with only the EDMD phenotype.

A previously described 2½-year-old boy had a condition resembling LGMD with contracture of the right ankle joint requiring Achilles tendon lengthening; this patient had an absence of emerin and had a mutation in *EMD*.[10] Both patients described herein demonstrated proximal muscle weakness with minimal or no joint contractures due to mutations in *EMD*. Patient 1 showed proximal muscular dystrophy without joint contractures and demonstrated only minimal cardiac involvement as transient sinus arrhythmia. However, joint contractures and a severe cardiac condition may develop in this patient. Patient 2 had unusual clinical findings manifesting as adult-onset LGMD. Minimal joint contractures were noticed only after careful physical examination at the age of 50 years. A conduction defect was observed during the course of his cardiac follow-up for valvular insufficiency. It remains unclear whether the absence of emerin has a role in the development of valvular insufficiency observed in this patient. The same mutation identified in patient 2 was previously reported in a patient with typical EDMD.[11] Additional unknown factors may cause different clinical phenotypes in patients harboring identical mutations in the same gene.

Based on these findings, mutations in *EMD* may cause the clinical phenotype of LGMD and the overlapping state of LGMD and EDMD, as seen in patients with mutations in *LMNA*. Cardiac involvement is the most important clinical symptom among patients with *EMD* mutations. Lethal conduction defects with cardiomyopathy have been observed not only in male patients but also in female carriers, at an older age compared with male patients.[12] Careful follow-up of cardiac function is essential, including female family members of patients even in the absence of overt clinical signs or the unavailability of genetic information. Diagnosis of emerin deficiency can be easily performed by immunohistochemical analysis using several tissue specimens. Our results demonstrate the importance of identifying emerin deficiency in patients with LGMD to provide prompt cardiac intervention and to avoid unexpected sudden cardiac death.

Accepted for Publication: December 13, 2006.
Correspondence: Yukiko K. Hayashi, MD, PhD, Department of Neuromuscular Research, National Institute of Neuroscience, National Center of Neurology and Psychiatry, 4-1-1 Ogawa-Higashi, Kodaira, Tokyo 187-8502, Japan (hayasi_y@ncnp.go.jp).
Author Contributions: *Study concept and design:* Ura, Hayashi, Ohta, and Nishino. *Acquisition of data:* Ura, Hayashi, Goto, Astejada, Murakami, Nagato, Ohta, Daimon, Takekawa, and Hirata. *Analysis and interpretation of data:* Ura, Hayashi, Nonaka, Noguchi, and Nishino. *Drafting of the manuscript:* Ura, Nagato, Ohta, Daimon, Takekawa, Hirata, and Noguchi. *Critical revision of the manuscript for important intellectual content:* Hayashi, Goto, Astejada, Murakami, Nonaka, and Nishino. *Obtained funding:* Hayashi and Nishino. *Administrative, technical, and material support:* Hayashi, Goto, Nonaka, and Noguchi.

Study supervision: Daimon, Takekawa, Hirata, and Nonaka.

Financial Disclosure: None reported.

Funding/Support: This study was supported in part by grants from the Human Frontier Science Program and by Research on Health Sciences focusing on Drug Innovation from the Japanese Health Sciences Foundation; by Research on Psychiatric and Neurological Diseases and Mental Health of Health and Labor Sciences Research Grants and Research Grant for Nervous and Mental Disorders from the Ministry of Health, Labor, and Welfare; by a Grant-in-Aid for Scientific Research from the Japan Society for the Promotion of Science; and by the Program for Promotion of Fundamental Studies in Health Sciences of the National Institute of Biomedical Innovation.

REFERENCES

1. Emery AE. Emery-Dreifuss muscular dystrophy and other related disorders. *Br Med Bull.* 1989;45(3):772-787.
2. Bione S, Maestrini E, Rivella S, et al. Identification of a novel X-linked gene responsible for Emery-Dreifuss muscular dystrophy. *Nat Genet.* 1994;8(4):323-327.
3. Bonne G, Di Barletta MR, Varnous S, et al. Mutations in the gene encoding lamin A/C cause autosomal dominant Emery-Dreifuss muscular dystrophy. *Nat Genet.* 1999;21(3):285-288.
4. Yorifuji H, Tadano Y, Tsuchiya Y, et al. Emerin, deficiency of which causes Emery-Dreifuss muscular dystrophy, is localized at the inner nuclear membrane. *Neurogenetics.* 1997;1(2):135-140.
5. Nagano A, Koga R, Ogawa M, et al. Emerin deficiency at the nuclear membrane in patients with Emery-Dreifuss muscular dystrophy. *Nat Genet.* 1996;12(3):254-259.
6. Manilal S, Sewry CA, Man N, Muntoni F, Morris GE. Diagnosis of X-linked Emery-Dreifuss muscular dystrophy by protein analysis of leucocytes and skin with monoclonal antibodies. *Neuromuscul Disord.* 1997;7(1):63-66.
7. Mora M, Cartegni L, Di Blasi C, et al. X-linked Emery-Dreifuss muscular dystrophy can be diagnosed from skin biopsy or blood sample. *Ann Neurol.* 1997;42(2):249-253.
8. Muchir A, Bonne G, van der Kooi AJ, et al. Identification of mutations in the gene encoding lamins A/C in autosomal dominant limb girdle muscular dystrophy with atrioventricular conduction disturbances (LGMD1B). *Hum Mol Genet.* 2000;9(9):1453-1459.
9. Tagawa K, Ogawa M, Kawabe K, et al. Protein and gene analyses of dysferlinopathy in a large group of Japanese muscular dystrophy patients. *J Neurol Sci.* 2003;211(1-2):23-28.
10. Muntoni F, Lichtarowicz-Krynska EJ, Sewry CA, et al. Early presentation of X-linked Emery-Dreifuss muscular dystrophy resembling limb-girdle muscular dystrophy. *Neuromuscul Disord.* 1998;8(2):72-76.
11. Manilal S, Recan D, Sewry CA, et al. Mutations in Emery-Dreifuss muscular dystrophy and their effects on emerin protein expression. *Hum Mol Genet.* 1998;7(5):855-864.
12. Sakata K, Shimizu M, Ino H, et al. High incidence of sudden cardiac death with conduction disturbances and atrial cardiomyopathy caused by a nonsense mutation in the *STA* gene [published online ahead of print June 20, 2005]. *Circulation.* 2005;111(25):3352-3358. doi:10.1161/CIRCULATIONAHA.104.527184.

Human Molecular Genetics, 2007, Vol. 16, No. 15 **1884–1895**
doi:10.1093/hmg/ddm137
Advance Access published on June 13, 2007

Activation of MAPK in hearts of *EMD* null mice: similarities between mouse models of X-linked and autosomal dominant Emery–Dreifuss muscular dystrophy

Antoine Muchir[1,2], Paul Pavlidis[3,†], Gisèle Bonne[4,5,6], Yukiko K. Hayashi[7] and Howard J. Worman[1,2,*]

[1]Department of Medicine and [2]Department of Anatomy and Cell Biology and [3]Department of Biomedical Informatics, College of Physicians and Surgeons, Columbia University, New York, USA and [4]Institut National de la Santé et de la Recherche Médicale, U582, Institut de Myologie, Paris, France and [5]Université Pierre et Marie Curie-Paris 6, Faculté de médecine, Paris, France and [6]AP-HP, Groupe hospitalier Pitié-Salpêtrière, U.F. Myogénétique et Cardiogénétique, service de Biochimie Métabolique, Paris, France and [7]Department of Neuromuscular Research, National Institute of Neuroscience, National Center of Neurology and Psychiatry, Tokyo, Japan

Received April 25, 2007; Revised and Accepted May 18, 2007

Emery–Dreifuss muscular dystrophy (EDMD) is an inherited disorder characterized by slowly progressive skeletal muscle weakness in a humero-peroneal distribution, early contractures and prominent cardiomyopathy with conduction block. Mutations in *EMD*, encoding emerin, and *LMNA*, encoding A-type lamins, respectively, cause X-linked and autosomal dominant EDMD. Emerin and A-type lamins are proteins of the inner membrane of the nuclear envelope. Whereas the genetic cause of EDMD has been described and the proteins well characterized, little is known on how abnormalities in nuclear envelope proteins cause striated muscle disease. In this study, we analyzed genome-wide expression profiles in hearts from *Emd* knockout mice, a model of X-linked EDMD, using Affymetrix GeneChips. This analysis showed a molecular signature similar to that we previously described in hearts from *Lmna* H222P knock-in mice, a model of autosomal dominant EDMD. There was a common activation of the ERK1/2 branch of the mitogen-activated protein kinase (MAPK) pathway in both murine models, as well as activation of downstream targets implicated in the pathogenesis of cardiomyopathy. Activation of MAPK signaling appears to be a cornerstone in the development of heart disease in both X-linked and autosomal dominant EDMD.

INTRODUCTION

Emery–Dreifuss muscular dystrophy (EDMD) is an inherited disorder characterized by contractures of the elbows, Achilles' tendons and spine, slowly progressive wasting and weakness of skeletal muscles in a humero-peroneal distribution (1). Individuals with EDMD also suffer from cardiomyopathy with conduction defects that increases the risk of sudden death. Initially described as an X-linked inherited disorder, autosomal dominant and recessive forms of EDMD are also recognized, with the dominant form being most prevalent.

X-linked EDMD arises as a consequence of mutations in *EMD* on chromosome Xq28 (2). *EMD* encodes emerin, a ubiquitously expressed integral protein of the inner nuclear membrane (3,4). Emerin is composed of 254 amino acids in humans and has a 220 amino acid nucleoplasmic amino-terminal domain, a single transmembrane segment and a short luminal tail (5). Emerin binds to several nuclear proteins

*To whom correspondence should be addressed at: Department of Medicine, College of Physicians and Surgeons, Columbia University, 630 West 168th Street, 10 Floor, Room 508, New York, NY 10032, USA. Tel: +1 2123058156; Fax: +1 2123056443; Email: hjw14@columbia.edu
†Present address: UBC Bioinformatics Centre, University of British Columbia, Vancouver, Canada BC V6T 1Z4.

and these interactions may underlie various functions attributed to emerin, including regulation of gene expression, nuclear assembly during mitosis, cell cycle control and providing structural support to the nuclear envelope (6). More recently, emerin has also been shown to bind β-catenin and restrict its accumulation in the nucleus (7).

Autosomal EDMD arises from mutations in *LMNA* (8). *LMNA* encodes A-type nuclear lamins, of which lamin A and lamin C are the predominant somatic cell isoforms (9). Nuclear lamins are intermediate filament proteins that polymerize to form a meshwork of 10 nm diameter filaments on the inner aspect of the inner nuclear membrane called the nuclear lamina (10–13). Lamins function in maintaining nuclear architecture and organizing chromatin (14–17). Lamins may also have complex roles in linking the nucleus to the cytoskeleton (18) and in DNA synthesis and transcription regulation (19–21). Lamins interact with integral proteins in the inner nuclear membrane, including emerin, and provide anchorage sites for chromatin and structural support to the nuclear envelope (6,22–27).

Genetically engineered mouse models have been created to study the role of emerin and A-type lamins in the development of EDMD. *Lmna* knockout mice provided the first animal model of the disease (27). The null mice develop cardiomyopathy and regional skeletal muscle wasting reminiscent of human EDMD (27). Subsequently, knock-in mice that express A-type lamins with the H222P (28) and N195K (29) amino acid substitutions were created. Similar to *Lmna* knockout mice, homozygous knock-in animals develop features of human EDMD, including cardiomyopathy; however, heterozygous mice are apparently normal. In transgenic mice, cardiac overexpression of human lamin A M371K leads to heart damage, whereas similar overexpression of wild type human lamin A does not cause significant abnormalities (30). Melcon *et al.* (31) have generated *Emd* null mice, reporting that $Emd^{-/y}$ males are normal at birth and that their subsequent postnatal growth and locomotion are indistinguishable from wild type siblings. These investigators did not report cardiac pathology in $Emd^{-/y}$ mice. Hayashi and colleagues (32) also generated and characterized *Emd* knockout mice and reported that they have a normal growth rate and life span without marked muscle weakness or joint abnormalities but have subtle motor coordination abnormalities. These investigators demonstrated small vacuoles in cardiomyocytes of emerin-deficient mice and detected a slight prolongation of atrioventricular conduction time in $Emd^{-/y}$ mice greater than 40 weeks of age.

Despite the fact that the human genetics have been well described and that relevant animal models have been generated, little is known about how mutations in the genes encoding emerin and A-type lamins lead to striated muscle abnormalities. One strategy that could allow for the identification of molecular abnormalities underlying muscle pathology in animal models of EDMD is comprehensive expression analysis at the transcriptome level using microarrays. Using such methods, Melcon *et al.* (31) have shown that regenerating skeletal muscle from emerin-deficient mice have abnormalities in cell cycle parameters and delayed myogenic differentiation, which is associated with perturbations to transcriptional pathways regulated by the retinoblastoma and MyoD genes. Hence, abnormalities in satellite cell proliferation or differentiation may be responsible for aspects of the pathophysiology of skeletal muscle disease in EDMD by impairing the replacement of fibers. However, this molecular mechanism cannot readily explain cardiac muscle abnormalities, as replacement of cardiomyocytes and regeneration of cardiac tissue is not significant. We recently identified activation of mitogen-activated protein kinase (MAPK) signaling pathway in hearts from mice with the *Lmna* H222P mutation (33). This molecular pathway has been previously implicated in the development of cardiomyopathy and conduction defects (34,35). We now report the results of a genome-wide expression analysis in hearts from *Emd* knockout mice, in which we have identified common molecular alterations found in *Lmna* H222P knock-in mouse hearts, including activation of a MAPK pathway.

RESULTS

Gene expression profiling analysis in hearts from Emd knockout mice

We performed a comparative genome-wide RNA expression analysis in hearts from $Emd^{-/y}$ mice. These mice have mild motor dysfunction, slight prolongation of atrioventricular conduction time and structural fragility of myonuclei (32). We studied mice at 10 weeks of age, before any signs of cardiac dysfunction, to focus on genes with expressions primarily altered as a result of emerin-deficiency and not secondary to possible cardiac damage. At 10 weeks of age, histological analysis of cardiac muscle from $Emd^{-/y}$ mice does not reveal notable pathological changes compared to hearts from control mice (data not shown).

To analyze transcriptomes, we used Affymetrix Mouse Genome 430 2.0 Arrays, which contain 45 101 probes sets for known and predicted genes. We first examined similarities in transcription profiles between hearts from control ($n = 8$) and $Emd^{-/y}$ ($n = 6$) mice by hierarchical cluster analysis. The individual patterns of mRNA signal intensities fell into two distinct groups on a heat map corresponding to the sample genotype, wild type and $Emd^{-/y}$, with similarity between members within each group higher than between the groups (Fig. 1A). This demonstrated that the differences in the distribution of mRNA expression intensities between heart tissue samples from wild type controls and $Emd^{-/y}$ mice were due to changes in the individual gene expression between groups rather than non-specific variations between samples. We then used a supervised learning method to distinguish probe sets representing genes with significant differences in expression between hearts from control and $Emd^{-/y}$ mice. Genes were selected using sufficiently high absolute changes measured by a corrected *t*-test ($q < 0.05$) combined with a one $\log_2$-fold change cut-off. This analysis identified 27 probe sets in hearts from $Emd^{-/y}$ mice, which correspond to 18 upregulated genes and 9 down-regulated genes (Fig. 1B).

The 27 genes with significant differences in expression in hearts of $Emd^{-/y}$ mice compared to control mice are listed in Table 1. Expression of *Emd* encoding emerin was significantly downregulated (1.8 $\log_2$-fold). Several muscle-specific genes were abnormally expressed in hearts from $Emd^{-/y}$ mice.